THE USE OF PORE SCALE MODELING TO PREDICT RESERVOIR PARAMETERS FROM DRILL CUTTINGS

Alex Mock[1], Pål-Eric Øren[1], Håkon Rueslåtten[1], Elin Rein[2], Sverre Henriksen[3]
[1]Numerical Rocks AS, [2]Norsk Hydro, [3]Statoil ASA

This paper was prepared for presentation at the International Symposium of the Society of Core Analysts held in Calgary, Canada, 10-12 September, 2007

ABSTRACT

This work investigates the use of an integrated pore-scale modeling procedure to determine reservoir rock parameters from drill cuttings. Our approach is based on reconstructing digital 3D models of reservoir rocks with input data obtained from drill cuttings. A variety of cuttings were investigated, ranging from chips several millimeters in size produced by conventional drill bits to a mixture of disintegrated sand grains and drilling mud produced by modern PDC drill bits. Different sample preparation methods were employed to analyze and extract petrographical information (porosity, mineralogy, and grain sizes) from the cuttings. Data derived from thin section analysis was supplemented by X-ray diffraction analysis (XRD), sieving and porosity logs. This information was used as input to a process based reconstruction algorithm to generate 3D models of the rock microstructure. Effective properties that are numerically calculated directly from the reconstructed models are absolute permeability, electrical resistivity, NMR relaxation, and elastic moduli. Relative permeability and capillary pressure curves are calculated on the pore network representations of the reconstructed rocks. Where data are available, computed properties are compared with data from well logs and laboratory measurements. In conclusion, this study shows that integrated pore-scale modeling offers exciting possibilities for estimating reservoir rock properties from drill cuttings.

INTRODUCTION

Drill cuttings are real samples of reservoir rocks and are often the only source of rock samples from drilled intervals in wells. Many attempts have been made to obtain petrophysical information from drill cuttings, but relative permeabilities and capillary pressures have not been measured on cuttings. Density and porosity have been reliably obtained (Siddiqui et al, 2005), and NMR techniques have been employed to predict permeabilities and pore-size distribution from drill cuttings (Mirotchnik et al, 2004). Laboratory methods have been developed to determine representative values of P- and S-wave velocities, elastic properties, residual fluid content and concentration (Santarelli et al, 1998). A direct laboratory method to measure permeability on drill cuttings is also available (Egerman et al, 2005). The reliability of these data depends strongly on the size of the chips produced by the drill bit. It has been suggested that chip sizes of 27 mm^3 are sufficient to predict meaningful petrophysical and mineralogical information (Fens et al, 1998).

In this work, an integrated pore-scale modeling procedure is used to determine petrophysical and multiphase properties from drill cuttings. The procedure involves three major steps:

1. Generation of 3D numerical rock models based on input data from thin section images;
2. Calculation of petrophysical properties on the grid representation of the rock model;
3. Extraction of the pore network and calculation of multiphase flow properties using network modeling techniques.

Detailed descriptions of the procedure have been presented before (e.g. Øren and Bakke, 2003) and will not be repeated here. The main focus in this work is to investigate the possibility of using drill cuttings to obtain petrographical information required to generate representative 3D rock models which can then be used to compute reservoir rock properties.

SAMPLES, PREPARATION AND ANALYSIS

Four different samples of highly different quality were investigated:

- **Sample 1 and 2**: totally disintegrated reservoir sandstone mixed with drilling mud and hydrocarbons, drilled with PDC drill bits (Figures 1 and 2).
- S**ample 3 and 4**: cleaned and dried cuttings with chip sizes up to 1mm (Figures 3 and 4).

Samples 1 and 2 required cleaning to remove hydrocarbons. These samples were also sieved with sieve size intervals of one phi. Sieve fractions <63µm and <4µm were analyzed with XRD. All samples were randomly embedded in blue-dyed epoxy resin under vacuum for the preparation of thin sections. All thin sections were imaged with a scanning electron microscope (SEM). Image analysis techniques were used to extract grain sizes and mineralogy from SEM images.

COMPUTED PROPERTIES

Permeability: The low Reynolds number flow of an incompressible Newtonian fluid is governed by the steady state Stokes equations

$$\mu\nabla^2\mathbf{v} = \nabla p\,, \tag{1}$$

$$\nabla\cdot\mathbf{v} = 0 \tag{2}$$

subject to the boundary condition $\mathbf{v} = 0$ on the solid walls. $\mathbf{v}$ and p are the velocity and pressure, respectively. A D3Q19 Lattice Boltzmann algorithm was used to solve the Stokes equations directly on the rock models. The macroscopic flux is found by volumetric averaging of the local velocities and the permeability k is determined from Darcy's law.

Formation Factor: For steady state conductivity problems, the governing local equations is the Laplace equation

$$\nabla \cdot \mathbf{J} = 0 \tag{3}$$

$$\mathbf{J} = \sigma_w \nabla \Phi \tag{4}$$

subject to the boundary condition $\nabla \Phi \cdot \mathbf{n} = 0$ on the solid walls. **J** is the electrical current, σ_w is the electrical conductivity of the fluid that fills the pore space, Φ is the potential or voltage, and **n** is the unit vector normal to the solid wall. Numerical solutions of the Laplace equation were obtained by a finite difference method (Øren and Bakke, 2002). The formation factor F is defined as the inverse of the effective conductivity $F = \sigma_w/\sigma$.

Elastic Moduli: The local equations that govern the elastic behaviour of the heterogeneous media are the basic equations of elastostatics

$$\nabla \cdot \tau = 0 \tag{5}$$

$$\tau = \mathbf{C} : \varepsilon \quad \text{with} \quad \varepsilon = \frac{1}{2}\left[\nabla \mathbf{d} + (\nabla \mathbf{d})^T \right] \tag{6}$$

where τ and ε denote the stress and strain tensors, respectively, **d** is the displacement field, and **C** is the stiffness tensor. The above equations were solved via a finite element method using an energy representation of the linear elastic equations. The effective bulk and shear moduli are computed assuming isotropic linear elastic behavior. Values used for individual mineral phases are reported in Table 3.

NMR Relaxation: The spin relaxation in NMR response of a saturated rock can be derived via solution of the diffusion equation in the pore space

$$\frac{\partial M}{\partial t} = D\nabla^2 M - \frac{M}{T_{2b}} \tag{7}$$

subject to the boundary condition $D\mathbf{n}\nabla M + \rho M = 0$ at the pore-solid interface. D denotes the self-diffusion coefficient, T_{2b} is the bulk transversal relaxation time of the fluid that fills the pore space, and ρ is the surface relaxation strength. The diffusion equation is solved by a random walk technique (Øren *et al.*, 2002). The magnetization amplitude, *M(t)*, is computed from the life time distribution of the walkers. The T_2 distribution curve is obtained by fitting a multi-exponential decay to the simulated *M(t)* curve.

Constitutive Relationships: Constitutive relationships, such as capillary pressure and relative permeability curves, are determined by simulating two-phase displacements (e.g., primary drainage, waterflood, secondary drainage) on the pore network representation of the computer generated rocks (Øren and Bakke, 2003). Since the extracted pore network is in a one-to-one correspondence with the reconstructed pore space, no fitting or tuning parameters are introduced to match macroscopic parameters such as porosity and permeability. In all the multiphase flow simulations it is assumed that capillary forces

dominate at the pore scale. A clear and comprehensive discussion of all the mathematical details involved in the simulations has been presented before (Øren *et al*., 1998, Øren and Bakke, 2003). In this work, primary drainage oil-water displacements were simulated on all the extracted pore networks. Fluid properties used for the simulations were: interfacial tension: 30mN/m, densities: 1000kg/m^3 (water), 700kg/m^3 (oil). Receding contact angles were randomly distributed between 0-30°.

RESULTS AND DISCUSSION

Input Data and Reconstructed Rock Models

For samples 1 and 2, grain size distributions both from sieving and image analysis show fractal trends characteristic of distributions produced by disintegration and crushing processes. Therefore, grain size distributions are a result of the drilling process and do not represent original size distributions. A normal distribution model is then used with the parameters reported in Table 1 and cut-off sizes (min/max) obtained from sieving and image analysis. From chips of samples 3 and 4, grain sizes were measured by image analysis of SEM images of several chips. It was not possible to measure a statistically significant number of grains. Therefore, the results were also used in a normal distribution model the parameters of which are reported in Table 1.

Results of XRD analysis were used to better estimate the mineralogy: content of different clay minerals, micas, feldspar content and abundance of carbonate cements. These results are affected by contamination with drilling mud. However, by combining image analysis results of several chips with results of sieving and XRD analysis, reasonable statistics for input parameters to the rock modeling procedure can be obtained.

The petrographical data, which are used as input for the geologically based reconstruction of the rock models, are summarized in Table 1. A range of values for one parameter indicates minimum and maximum values used in different model realizations. In addition to data from the samples themselves, information from porosity logs were used to anchor the models.

The generated models are cubes with side lengths between 4 and 7.6mm, containing between 800^3 and 950^3 grid cells (voxels). The models consist of between 10^4 to $4x10^4$ virtual sand grains. Each model constitutes an REV of their respective inferred grain size distribution and porosity as can be shown by calculating their two-point correlation functions. The decay length can be assumed to be 10% of the side length of an REV. However, two-point correlation functions of the models cannot be compared directly with images of the samples because individual chips do not constitute an REV. PDC bits do not produce chips of the original rock at all (samples 1 and 2). In addition, information about heterogeneities in the rock (laminations, patchy cementation, vugs etc.) cannot be obtained reliably from the cuttings samples and are, thus, not represented in the models. However, these structures can be responsible for long correlation lengths.

Petrophysical Properties

Permeability was calculated on each model realization. Results and measured permeabilities are reported in Table 2. Measured and modeled permeabilities compare reasonably well (with one exception within an order of magnitude). This is very encouraging, especially in the light of large uncertainties in sample porosity and composition.

Formation factors and effective bulk and shear moduli were calculated on each realization of a sample. Average values are reported in Table 2. Elastic properties can be used to calculate seismic velocities (V_P and V_S). Electrical properties should be compared to resistivity logs. However, no data were available for comparison.

NMR relaxation was calculated on each model realization assuming a fully brine saturated sample. Results of NMR simulations are shown in Figure 5. The calculations were performed using typical parameters for brine saturated sandstones: $\rho = 18 \mu m/s$ and $D = 3300 \mu m^2/s$ (Øren *et al*., 2002). The T2 relaxation time for water saturated sandstones is largely governed by the pore size distribution. Peaks in the interval 400 to 900ms correspond to rather large pore sizes, while the faster relaxing water is situated in the intermediate and small pore size classes (Figure 5). A microporosity of 50% is attributed to clays in the rock models, and water relaxing faster than 30ms is attributed to this clay bound water. Variation in clay content for the different model realizations (Table 1) changes the location and amplitudes of NMR peaks corresponding to this fast relaxing water (Figure 5). Unfortunately, no measured NMR data were available for comparison.

Multiphase Properties

The computed primary drainage capillary pressure and relative permeability curves for the different samples are shown in Figures 6 and 7, respectively. The irreducible water saturations are listed in Table 2. Experimental data for comparison were not available. However, data from neighboring cored wells might be used for comparison if core samples have the same properties. The predicted capillary pressures and relative permeabilities of sample 4 compare well with results of models based on thin sections of two core plugs from a nearby well of similar formation and rock type (see Figures 6 and 7).

Sampling Uncertainties

Generally, cuttings are sampled routinely once every 3 to 10m, which causes a low accuracy in depth determination. The presence of clear geological markers will facilitate the tie-in with well logs (LWD or wireline logs). The drill cuttings may also be ‘contaminated’ with cuttings from earlier drilled formations, which may be difficult to identify. In addition, fine scale structures such as laminations, mud drapes etc. cannot be recognized reliably and incorporated into the models. This should be kept in mind when comparing the cuttings data with well logs or core analysis from neighboring wells.

CONCLUSIONS

- An integrated pore-scale modeling procedure was used to determine reservoir rock parameters from drill cuttings obtained from both PDC and conventional drill bits.
- By combining sieving, XRD, SEM and image analysis, relevant input data for numerical rock models can be obtained. Data from wireline logs, e.g. porosity, can be included in the modeling routine where the cuttings alone leave too much uncertainty.
- Predicted permeabilities agree reasonably well with measured data.
- NMR relaxation, electric, elastic and multiphase flow properties were calculated, but could not be compared with experimental data.
- The main uncertainties in the modeling procedure are related to sampling accuracy, drill bit used, and cleaning methods. Additionally, structures responsible for long range correlations such as laminations, patchy cementation and vugs are difficult to capture in cuttings samples.
- Integrated pore-scale modeling can provide relevant reservoir data where cores are not available. However, more experience must be gained by working with a larger number and variety of drill cuttings samples and getting access to high quality SCAL data for comparison. Therefore, this study must be regarded as a pilot study to investigate the use of integrated pore-scale modeling for drill cuttings.

References

Bakke, S., Øren, P.-E., "3-D pore-scale modelling of sandstones and flow simulations in the pore networks," *SPE Journal*, (1997) **2**, 136-149.

Egerman, P., Lenormand, R., Longeron, D. and Zarcone, C., "A fast and direct method of permeability measurement on drill cuttings," *SPE Reservoir Evaluation & Engineering*, (2005) **8,** 4, 269-275.

Fens, T. W., Kraaijveld, M. A., Riepe, L., Visser, R., "Archie's dream: petrophysics from sidewall samples and cuttings," *SCA*, (1998), 9805.

Mirochtnik, K., Kryuchkov, S., Strack, K., "A novel method to determine NMR petrophysical parameters from drill cuttings," *SPWLA 45th Annual Logging Symposium, Noordwijk, Netherlands*, (2004).

Øren, P.-E., Bakke, S., Arntzen, O. J., "Extending predictive capabilities to network models," *SPE Journal* (1998) **3**, 324-336.

Øren, P.-E., Bakke, S., "Process based reconstruction of sandstones and predictions of transport properties," *Transport in Porous Media*, (2002) **46**, 311-343.

Øren, P.-E., Antonsen, F., Rueslåtten, H., Bakke, S., "Numerical simulations of NMR responses for improved interpretations of NMR measurements in reservoir rocks," *SPE paper 77398, SPE Annual Technical Conference and Exhibition, San Antonio, Texas*, (2002).

Øren, P.-E., Bakke, S., "Reconstruction of Berea sandstone and pore-scale modelling of wettability effects," *Journal of Petroleum Science & Engineering*, (2003) **39,** 177-199.

Santarelli, F. J., Marsala, A. F., Brignoli, M., Rossi, E., Bona, N., "Formation evaluation from logging on cuttings," *SPE Reservoir Evaluation & Engineering,* (1998) **1**, 3, 238-244.
Siddiqui, S., Grader, A. S., Touati, M., Loermans, A. M., Fun, J. J., "Techniques for extracting reliable density and porosity data from cuttings," *SPE Annual Technical Conference, Dallas, Texas,* (2005), 96918.

Acknowledgements
Russell Watson at ResLab, Trondheim, performed sample cleaning. His contribution is thankfully acknowledged. We thank Norsk Hydro and Statoil ASA for permission to publish these results.

Tables and Figures
Table 1. Input data derived from sieving, image analysis of thin sections, XRD and logs. Ranges give variation for different model realizations of the same sample. Values are volume fractions if not otherwise stated. Grain size data refer to a normal grain size distribution model with cut-off (min/max) obtained from sieving and image analysis.

	Sample 1	Sample 2	Sample 3	Sample 4
Porosity (total)	0.25 – 0.31	0.26 – 0.31	0.11 – 0.14	0.12 – 0.15
Porosity (intergran.)	0.19 – 0.23	0.11 – 0.17	0.09 – 0.13	0.12 – 0.13
Mean Grain Size [µm]	200 – 350	75 – 150	70	75 – 150
Max Grain Size [µm]	500 – 750	700	450	350 – 500
Min Grain Size [µm]	44	44	70	30 – 75
St.dev. Grain Size	100 – 250	100 – 300	80 – 150	40 – 100
Clay	0.1 – 0.14	0.1 – 0.2	0.02 – 0.04	0.05
Feldspar	0.02 – 0.05	0.05	<0.02	0.02 – 0.04
Mica	0.005	0.01	---	0.005
Carbonate Cement	0.06	0.024	0.0025	---
Other Cement	0.001	0.012	0.0025	0.0001

Table 2. Petrophysical properties calculated on models of cuttings samples; averages from all model realizations. Measured permeabilities and porosity ranges stem from logs and core analysis data of neighboring wells in the same formation and corresponding depth interval.

	Sample 1	Sample 2	Sample 3	Sample 4
Porosity range (log)	0.18 – 0.26 [c]	<0.1 – 0.24 [c]	0.08 – 0.16 [c]	0.14 – 0.25 [c]
Measured Perm. (log) [mD]	500 – 600[a]	~1000 [a]	0.2 [a]	109 – 322 [b]
Calc. Perm. [mD]	2000 – 4000	94 – 205	15 – 160	21 – 131
Formation Factor	21	57	55	58
Bulk modulus [GPa]	19.3	31.5	24.5	Not calculated
Shear modulus [GPa]	18.2	29.3	25.6	Not calculated
Swi (Primary Drainage)	0.23	0.25 – 0.5	0.15 – 0.3	0.22 – 0.33

[a] from permeability log; [b] SCAL data; [c] He-porosities

Table 3. Bulk and shear moduli of individual mineral phases used in the calculation of effective bulk and shear moduli of rock models.

	Clay	Quartz	Mica	Feldspar	Carbonate	Pyrite
Bulk [GPa]	50.0	37.0	58.2	65.0	73.3	142.7
Shear [GPa]	30.0	44.0	35.3	30.0	30.0	125.7

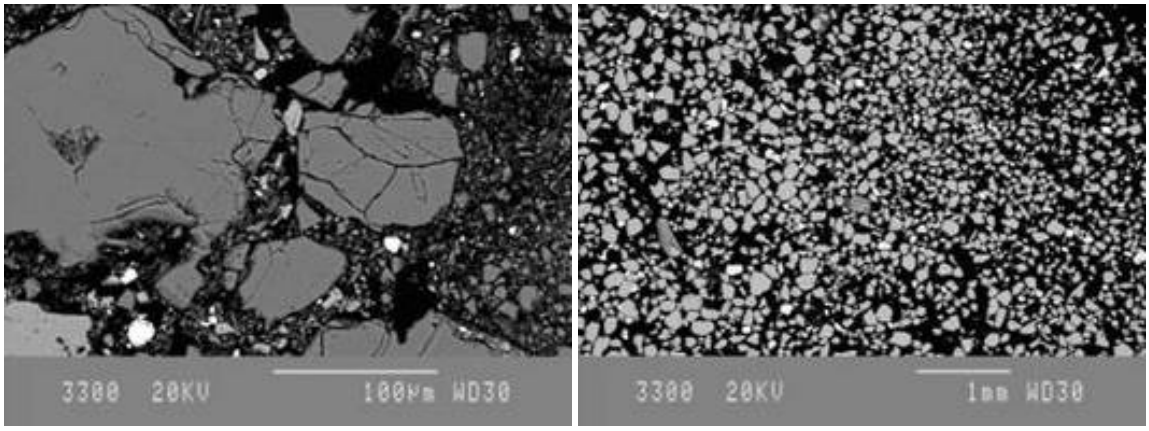

Figure 1: Detail of **sample 1** showing broken quartz grains and very fine grained quartz embedded in a clay matrix (on the right), possibly crushed grains mixed with drilling mud. Grains of **sample 1** after cleaning with HCl; only single quartz grains are preserved which often show concave edges indicating that grains have been crushed.

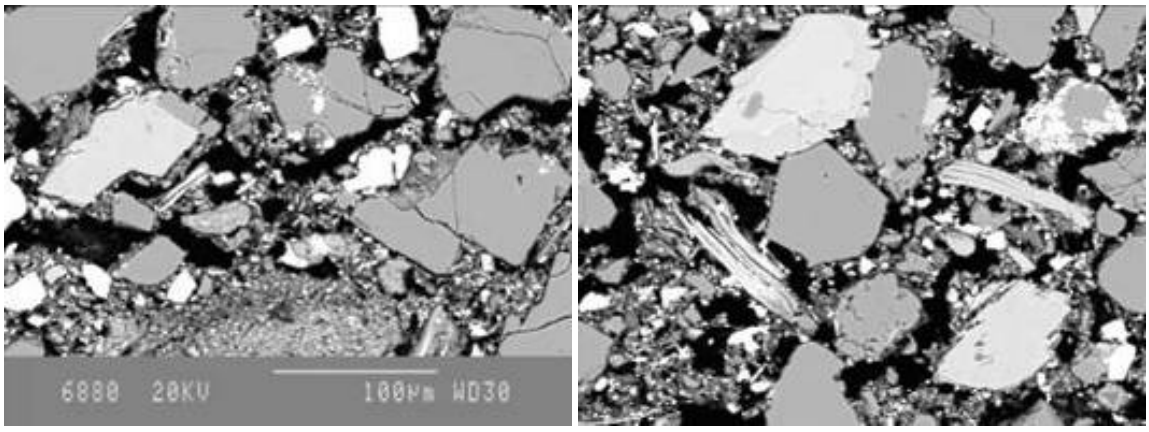

Figure 2. Details of **sample 2**: note high abundance of clay (darker grey) and large white grains, which are most likely barite from the drilling fluid. Quartz grains show unusual shapes (concave edges) and are generally not in contact with each other. Image on the right has same scale and shows some mica grains.

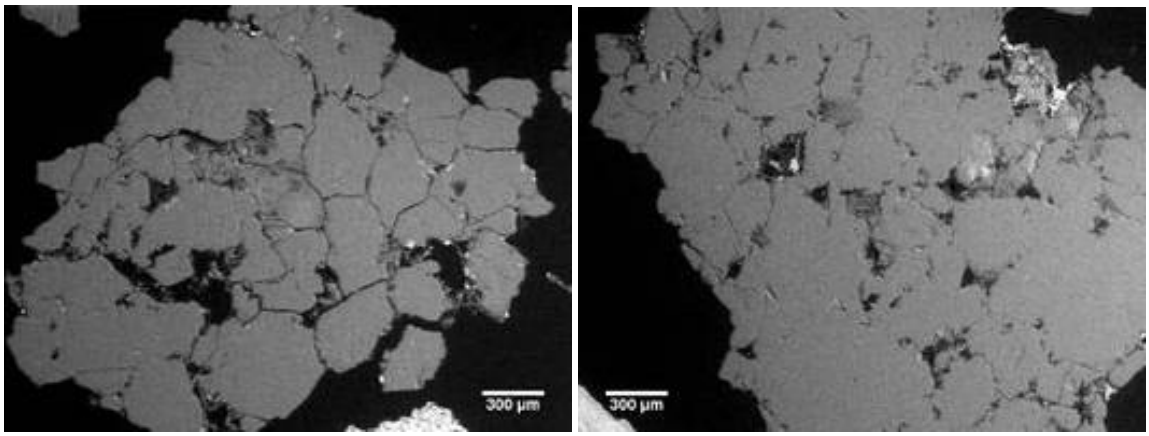

Figure 3. Two chips of **sample 3**: the original texture of the reservoir rock is well preserved. About 400 grains could be identified from six such chips. Note low intergranular porosity (mostly quartz cement, minor clay), partly dissolved feldspars.

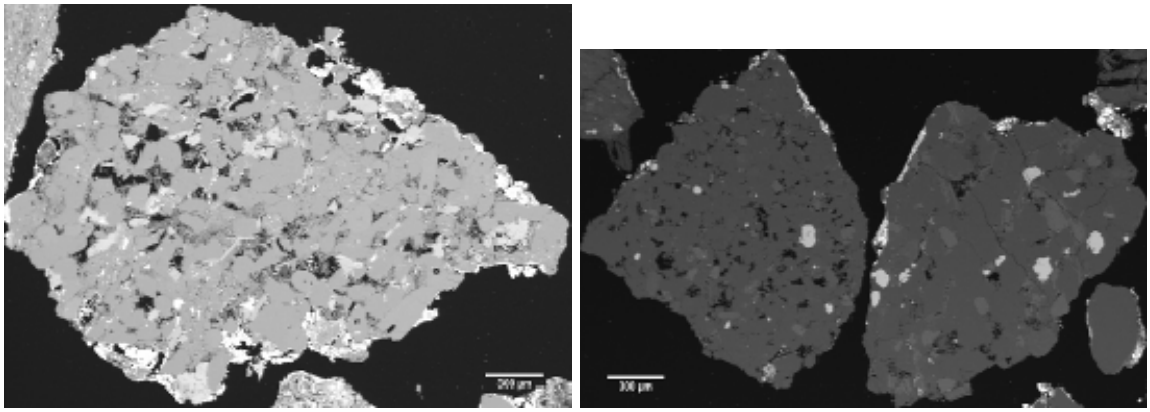

Figure 4. Three chips of **sample 4** showing relatively well preserved rock texture, well recognizable grains, high clay content and possible contamination of drilling mud (bright phases partly invading the pore space.

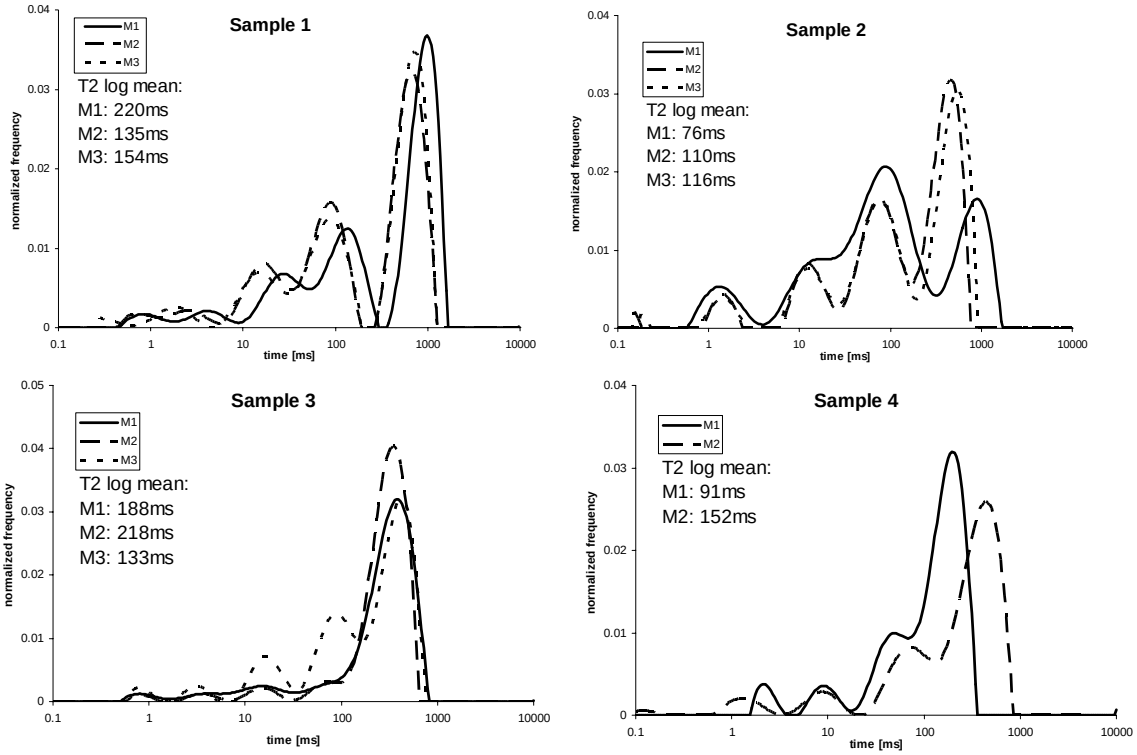

Figure 5. NMR T2 distribution curves of modeled samples. Different curves in one diagram correspond to different model realizations of one sample (M1, 2, 3…).

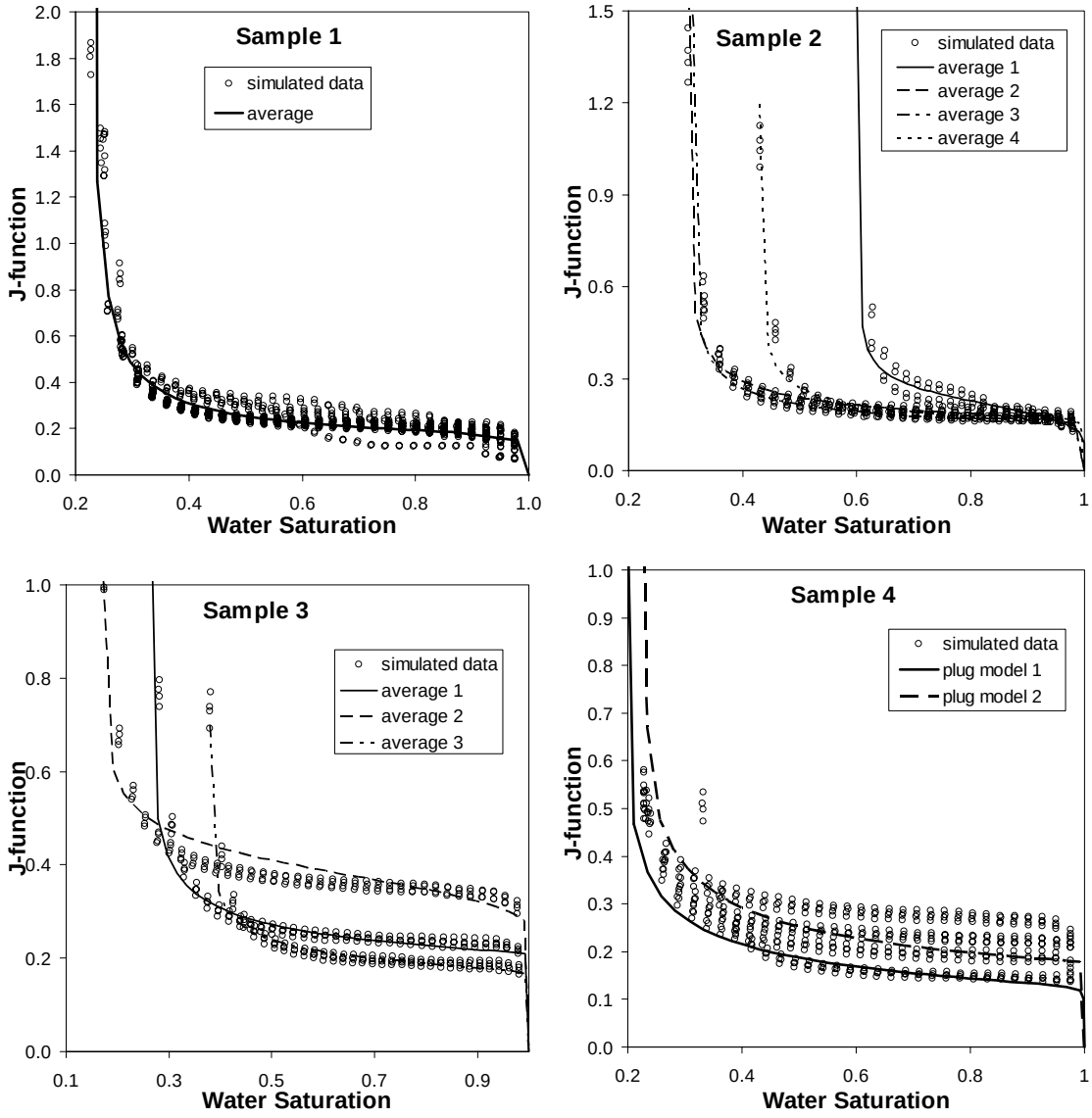

Figure 6. Capillary pressure curves resulting from e-Core models plotted as Leverett-J-function. Note different S_{wi} for samples 2 and 3 due to variation in microporous clay content. Samples 3 and 5 show more scatter in simulated data because of variation in grain size distributions.

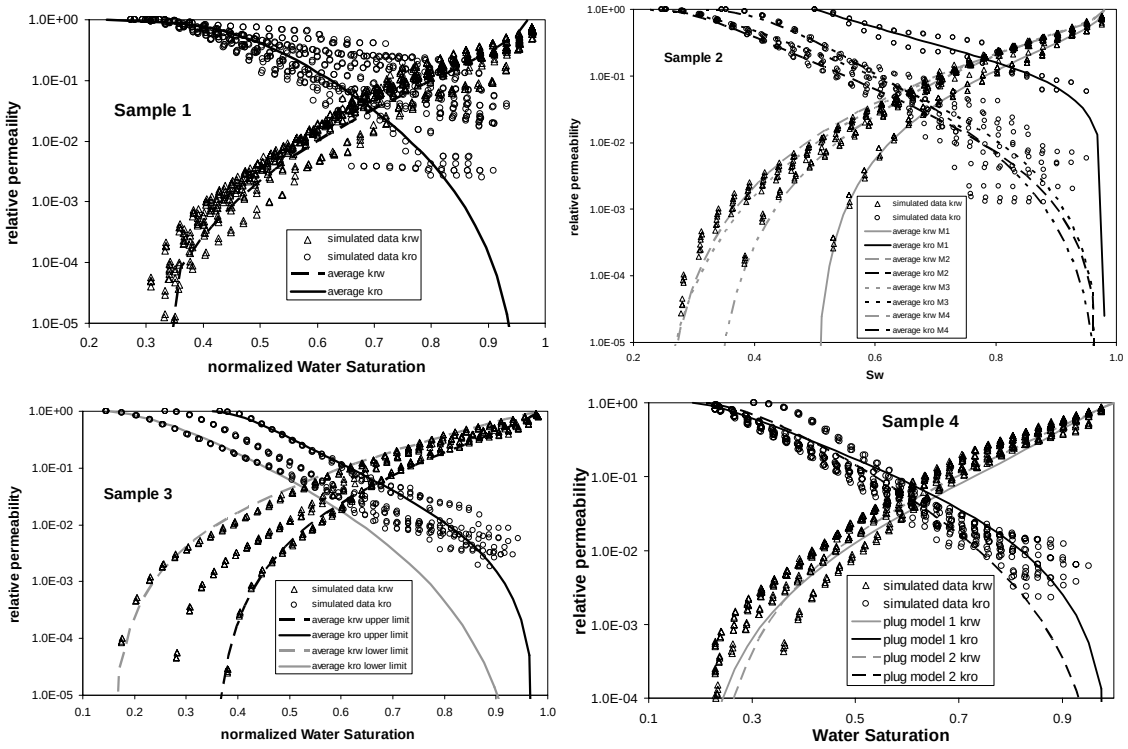

Figure 7. Relative permeability curves obtained from all model realizations of each sample.